IL NUOVO CIMENTO Vol. 32 C, N. 1 Gennaio-Febbraio 2009
DOI 10.1393/ncc/i2009-10334-7

Colloquia: GCM8

A micromechanically motivated model for the viscoelastic behaviour of soft biological tissues at large strains

A. E. Ehret, M. Itskov and G. W. Weinhold
Department of Continuum Mechanics, RWTH Aachen University - 52056 Aachen, Germany

(ricevuto il 3 Aprile 2009; pubblicato online il 20 Maggio 2009)

Summary. — In this contribution, a non-linear viscoelastic anisotropic model for soft biological tissues is presented. The viscoelastic behaviour of these materials is explained by micromechanical considerations regarding the interplay between collagen fibres and the surrounding ground substance. The model is based on a multiplicative decomposition of the fibre stretch into a part relating to the straightening of the crimped fibres and a part describing the stretch in the fibre itself. The actual structural state of the fibres is reflected by internal variables. Including a non-uniform distribution of these fibres, the anisotropic three-dimensional constitutive equations are obtained by integration over the unit sphere. The model holds for large strain problems and is illustrated by application to arterial tissue.

PACS 46.05.+b – General theory of continuum mechanics of solids.
PACS 46.35.+z – Viscoelasticity, plasticity, viscoplasticity.

1. – Introduction

Soft biological tissues such as skin, tendons, ligaments or the components of the cardiovascular system are composite materials. From a mechanical point of view, the extracellular matrix surrounding the cells predefines the passive tissue characteristics to a large extent. It generally contains water-rich amorphous constituents, referred to as the ground substance, and fibrous components such as some collagen types, the spatial arrangement of which leads to anisotropic material properties.

In mechanical tests, soft biological tissues reveal stress relaxation when stretched to a constant level and rate-dependent hysteresis in cyclic loading. These and other viscoelastic effects depend on the direction of loading and are thus of anisotropic nature. In constitutive models, the viscoelastic behaviour has been accounted for by different approaches such as quasi-linear viscoelasticity (see [1]), the theory of internal variables (*e.g.* [2-6]), multi-phasic material laws (*e.g.* [7, 8]) and explicitly rate-dependent models (*e.g.* [9-11]). The non-linear anisotropic viscoelastic model presented and elaborated in this contribution is motivated by microstructural mechanisms during tissue deformation.

Precisely, the viscoelastic behaviour results from the resistance of the water-rich ground substance to a straightening of undulated fibres.

The contribution is organised as follows. The constitutive model is presented in sect. **2** and applied to arterial tissue in sect. **3**. Finally, sect. **4** summarises and concludes the paper.

2. – Constitutive model

2˙1. *Non-linear fibre-matrix interaction model.* – When soft biological tissues are stretched, they usually exhibit a J-shaped stress response, which can be divided into a toe, heel and linear region. This non-linear behaviour is explained by unfolding and gradual alignment of initially crimped collagen fibres which are finally characterised by linear behaviour when fully straightened (see *e.g.* [1]). Accordingly, stretching the tissue involves both fibre straightening and straining of the fibre material itself. In order to incorporate this mechanism in a constitutive model, the stretch λ along a fibre direction specified by the unit vector $\boldsymbol{a}$ is decomposed into a part λ_v associated with straightening and λ_e reflecting the stretching of the fibre as

$$\lambda = \sqrt{\mathrm{tr}(\mathbf{CA})} = \lambda_e \lambda_v, \tag{1}$$

where $\mathbf{C}$ denotes the right Cauchy-Green tensor and $\mathbf{A} = \boldsymbol{a} \otimes \boldsymbol{a}$ is a structural tensor. Introducing the strain-energy functions $\Psi_e(\lambda_e)$ and $\Psi_v(\lambda_v)$ associated with stretching and unfolding, respectively, the free energy is given by

$$\Psi(\lambda, \lambda_v) = \Psi_e(\lambda_e(\lambda, \lambda_v)) + \Psi_v(\lambda_v), \tag{2}$$

where the stretch λ_v is treated as an internal variable describing the current state of unfolding of the fibres. In order to guarantee an energy- and stress-free undeformed configuration, the functions on the right-hand side of (2) obey the conditions

$$\Psi_e(1) = \Psi_v(1) = 0, \qquad \Psi_e'(1) = \Psi_v'(1) = 0, \tag{3}$$

where the prime denotes the derivative. The fibres are embedded in the surrounding water-rich material referred to as ground substance, which undergoes rearrangement if the fibres unfold. The resistance of this viscoelastic matrix controls the degree of fibre straightening in the model. This idea is supported by recent experiments on tendon tissue [12]. Accordingly, the extension of a fibril is "considerably less" than that of the tendon and the ratio between fibril and tendon extension increases with strain rate due to a stiffening of the proteoglycan-rich matrix [12]. The rate of entropy production $\mathcal{D}$ associated with stretching of the fibre-matrix compound is expressed by the Clausius-Duhem inequality in the one-dimensional form

$$\mathcal{D} = P\dot{\lambda} - \dot{\Psi} \geq 0, \tag{4}$$

where P is the fibre nominal stress, which is energy-conjugate to the fibre stretch λ. Inserting (2) into (4), applying the chain rule of differentiation and using basic statements

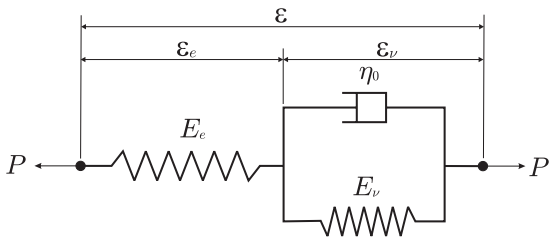

Fig. 1. – Standard three-parameter rheological model for small strains, which results from the proposed non-linear large strain model by linearisation.

of thermodynamics, one obtains the fibre nominal stress and the reduced dissipation inequality as [13]

$$P = \frac{\partial \Psi_e}{\partial \lambda_e}\lambda_v^{-1}, \qquad \mathcal{D} = \left[\frac{\partial \Psi_e}{\partial \lambda_e}\lambda_e - \frac{\partial \Psi_v}{\partial \lambda_v}\lambda_v\right]\dot{\lambda}_v\lambda_v^{-1} \geq 0. \tag{5}$$

In order to guarantee a non-negative rate of entropy production, we set up the evolution equation

$$\dot{\lambda}_v = \frac{\lambda_v}{\eta(\lambda,\lambda_v)}\left[\frac{\partial \Psi_e}{\partial \lambda_e}\lambda_e - \frac{\partial \Psi_v}{\partial \lambda_v}\lambda_v\right] = \frac{\lambda_v T(\lambda,\lambda_v)}{\eta(\lambda,\lambda_v)}, \tag{6}$$

which yields a quadratic form in $(5)_2$, where $\eta(\lambda,\lambda_v)$ is a positive definite viscosity function controlling the resistance of the viscoelastic matrix against fibre unfolding. Note that the abbreviation $T(\lambda,\lambda_v)$ has been introduced as the driving force for the evolution of λ_v.

Due to the multiplicative decomposition (1) the constitutive model (5), (6) is applicable for large strain problems. Notwithstanding, linearising the nominal stress $(5)_1$ and the evolution equation (6) around $\lambda = 1$, $\lambda_v = 1$ and considering that $\lambda = 1 + \varepsilon$, $\lambda_v = 1 + \varepsilon_v$, the model reduces to a standard three-parameter solid (Zener model, fig. 1) for small strains, where $|\varepsilon_e| \ll 1$, $|\varepsilon_v| \ll 1$. In this case, Young's moduli of the spring elements and the viscosity of the dashpot in the linearised model are given by [13]

$$E_e = \left.\frac{\partial^2 \Psi_e}{\partial \lambda_e^2}\right|_{\lambda=\lambda_v=1}, \qquad E_v = \left.\frac{\partial^2 \Psi_v}{\partial \lambda_v^2}\right|_{\lambda=\lambda_v=1}, \qquad \eta_0 = \eta(1,1). \tag{7}$$

Consequently, the rheological scheme in fig. 1 serves as a useful illustration for the proposed large strain model.

2˙2. *Three-dimensional anisotropic model.* – Following the framework of Lanir [14], the one-dimensional model is generalised to the three-dimensional case by integration over the unit sphere. Accordingly, considering the spherical coordinates (φ,θ), the fibre direction unit vector $\boldsymbol{a}$ and the associated structural tensor $\mathbf{A}$ are given by

$$\mathbf{A}(\varphi,\theta) = \boldsymbol{a}(\varphi,\theta) \otimes \boldsymbol{a}(\varphi,\theta). \tag{8}$$

In general, the alignment of collagen fibres is spatially distributed. In order to reflect such a non-uniform arrangement in the tissue, a distribution function $\Phi(\varphi,\theta)$ is considered, which satisfies the normalisation condition $\int_\Omega \Phi \,\mathrm{d}\Omega = \frac{1}{4\pi}\int_{-\pi}^{\pi}\int_0^{\pi} \sin\theta \mathrm{d}\theta\mathrm{d}\varphi = 1$. Accordingly, the overall free energy is obtained by integration

$$W = \mu \int_\Omega \Phi(\varphi,\theta)\Psi(\lambda(\varphi,\theta),\lambda_v(\varphi,\theta))\,\mathrm{d}\Omega, \tag{9}$$

where μ is the fibre density describing the number of fibres per unit volume. Since, in general, the latter integral does not allow for an analytical solution, Gaussian quadrature stands to reason. Accordingly, considering n integration points with coordinates (φ_i,θ_i) on the surface of the unit sphere and the associated weights B_i, $i = 1,2,\ldots,n$, $\sum_{i=1}^{n} B_i = 1$, the integral (9) turns into

$$W = \mu \sum_{i=1}^{n} B_i \Phi_i \Psi(\lambda^i, \lambda_v^i), \tag{10}$$

where $\Phi_i = \Phi(\varphi_i,\theta_i)$, $\mathbf{A}_i = \mathbf{A}(\varphi_i,\theta_i)$, $\lambda^i = \sqrt{\mathrm{tr}(\mathbf{C}\mathbf{A}_i)}$ and $\lambda_v^i = \lambda_v(\varphi_i,\theta_i)$. In analogy to (4) and (5), we insert the latter expression into the Clausius-Duhem inequality and obtain

$$\mathcal{D} = \left[\frac{1}{2}\mathbf{S} - \frac{\partial W}{\partial \mathbf{C}}\right] : \dot{\mathbf{C}} - \mu \sum_{i=1}^{n} B_i \Phi_i \frac{\partial \Psi(\lambda^i,\lambda_v^i)}{\partial \lambda_v^i}\dot{\lambda}_v^i \geq 0, \tag{11}$$

which defines the second Piola-Kirchhoff stress tensor $\mathbf{S}$ and motivates n evolution equations for λ_v^i in analogy to eq. (6) as

$$\mathbf{S} = \mu \sum_{i=1}^{n} B_i \Phi_i \frac{P(\lambda^i,\lambda_v^i)}{\lambda^i}\mathbf{A}_i, \qquad \dot{\lambda}_v^i = \frac{\lambda_v^i\, T(\lambda^i,\lambda_v^i)}{\eta(\lambda^i,\lambda_v^i)}\,. \tag{12}$$

Due to their high water content, soft biological tissues show very slight compressibility and are therefore often modelled as incompressible. Taking this constraint into account, we have

$$\mathbf{S} = \mu \sum_{i=1}^{n} B_i \Phi_i \frac{P(\lambda^i,\lambda_v^i)}{\lambda^i}\mathbf{A}_i - p\mathbf{C}^{-1}, \tag{13}$$

where p is a scalar associated with the hydrostatic pressure.

2˙3. *Issues of numerical integration on the sphere.* – Numerical integration on the sphere has frequently been used in constitutive modelling applications (*e.g.* [15,16]). We remark, however, that this operation is generally prone to induce large defects. In addition to the numerical error between the integral (9) and its approximate solution (10), the distribution of the integration points on the sphere can violate the original material symmetry of the constitutive equations [17]. Both deficiencies decrease with an increasing number of nodes and can be minimised by choosing the integration scheme appropriately [17]. To this end, in the present paper, an integration scheme characterised by central symmetry with 45 nodes on a hemisphere is utilised [17,18], which offers a good compromise between numerical accuracy and efficiency.

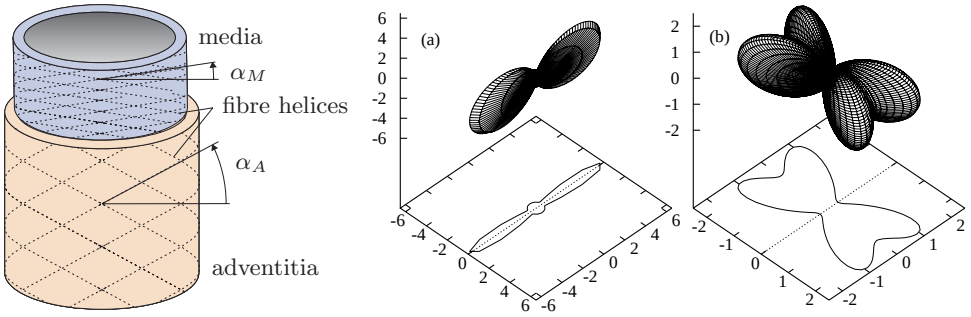

Fig. 2. – Arterial layers (left) and plots of the fibre distributions in the media (a) and adventitia (b) according to (16) (right). The dashed line in the distribution plots indicates the circumferential direction. Parameters: $b_A = 3.0$, $\alpha_A = 61.2°$, $g_A = 0.3$, $b_M = 20.0$, $\alpha_M = 3.6°$, $g_M = 0.6$.

3. – Numerical examples

In this section we define appropriate strain-energy, viscosity and distribution functions and illustrate the model in application to arterial tissue. The J-shaped stress-strain behaviour of arterial tissue is well described by exponential expressions [19] in combination with a linear model as

$$\Psi_e(\lambda_e) = \frac{c}{2}(\lambda_e - 1)^2, \qquad \Psi_v(\lambda_v) = \begin{cases} \frac{k_1}{2k_2}\left\{\exp\left[k_2(\lambda_v^2 - 1)^2\right] - 1\right\} & \text{if } \lambda_v \geq 1, \\ 0 & \text{else,} \end{cases} \tag{14}$$

where the material constants c, k_1 have the dimension of stress and k_2 is dimensionless (cf. [19]). The viscosity is assumed to increase with fibre straightening and is represented by the special case

$$\eta(\lambda, \lambda_v) = \bar{\eta}(\lambda_v) = \eta_0 \exp\left[d(\lambda_v - 1)^2\right] \tag{15}$$

with initial viscosity η_0 and a parameter d. The arterial wall consists of three distinct layers, referred to as tunica intima, media and adventitia. In the healthy artery, the latter two layers and in particular the media dominate the mechanical response and are characterised by helically arranged fibrous constituents (see, *e.g.*, [19] for details). In the media the fibre helices follow preferred directions which are nearly circumferentially aligned, whereas in the adventitia the arrangement of fibres is much less coherent [20] and can have a considerable pitch from the circumferential direction (fig. 2). The dispersion of the fibres from their mean directions are modelled by the distribution functions

$$\Phi_i = g_i + (1 - g_i)\frac{3\left(e^{b_i \cos[2(\varphi - \alpha_i)]} + e^{b_i \cos[2(\varphi + \alpha_i)]}\right)\sin^2(\theta)}{4I_0(b_i)}, \quad i = M, A, \tag{16}$$

where φ and θ are spherical coordinates such that $0 \leq \theta \leq \pi$ is the zenith angle measured from the radial direction of the artery and $0 \leq \varphi \leq 2\pi$ is the angle in the wall plane spanned by the axial and circumferential directions of the artery. $I_0(x)$ is the modified

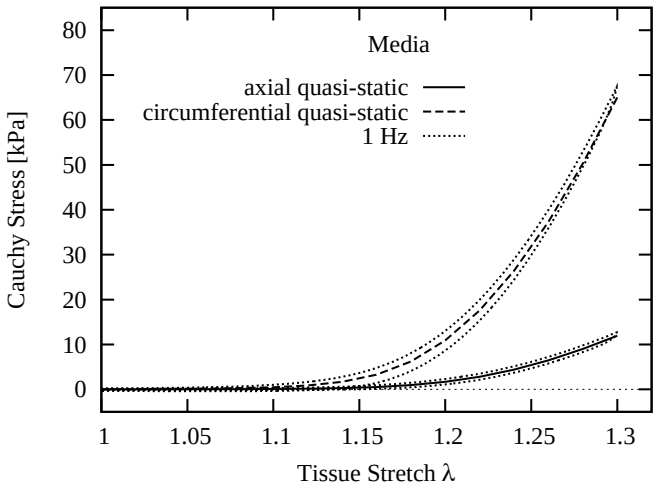

Fig. 3. – Cauchy stress *vs.* stretch for loading of medial tissue in axial and circumferential direction. The curves show the equilibrium responses and the solutions for stretch controlled triangular-shaped loading/unloading at 1 Hz. Anisotropy and hysteretic behaviour are observed. Material parameters: $\mu = 1.0$, $c = 2880.0\,\mathrm{kPa}$, $k_1 = 1.28\,\mathrm{kPa}$, $k_2 = 23.0$, $\eta_0 = 1.6\,\mathrm{kPas}$, $d = 100.0$.

Bessel function of order zero, α_i denotes the pitch of the preferred fibre orientations from the circumferential direction and b_i are parameters controlling the degree of dispersion. Note that function (16) is composed of scaled von-Mises distributions combined with a uniform base distribution g_i. The latter one guarantees some fibres in all directions. The fibre distributions in the media and adventitia are exemplified in fig. 2.

We simulate experiments in which tissue strips cut in longitudinal and circumferential direction are subject to uniaxial tension with quasi-static loading and stretch controlled triangular-shaped loading/unloading at a frequency of 1 Hz. The results are shown in figs. 3 and 4. In the quasi-static case, the driving force for an evolution of λ_v^i in $(12)_2$ vanishes, *i.e.* $T(\lambda^i, \lambda_v^i) = 0$, $i = 1, 2, \ldots, n$. The resulting equilibrium stress-stretch curves reveal the typical J-shaped response of fibrous tissues. Increasing the strain rate leads to hysteretic behaviour. Both the equilibrium and viscoelastic stress responses are characterised by strong anisotropy which is predefined by the fibre distribution (16) as depicted in fig. 2. Note that in this example, we normalised the parameter μ so that the material parameters c, k_1 and k_2 refer to the entire amount of fibres and not a single fibril.

4. – Conclusions

In the present contribution, a non-linear anisotropic model for the viscoelastic behaviour of soft biological tissues has been presented which is based on the interplay between collagen fibres and the surrounding ground substance. This microstructural interplay is taken into account by a one-dimensional rheological model, which simplifies to the classical three-parameter solid (Zener) model for infinitesimal strains. Including a non-uniform distribution of fibres, a fully three-dimensional anisotropic constitutive model is obtained by numerical integration over the unit sphere.

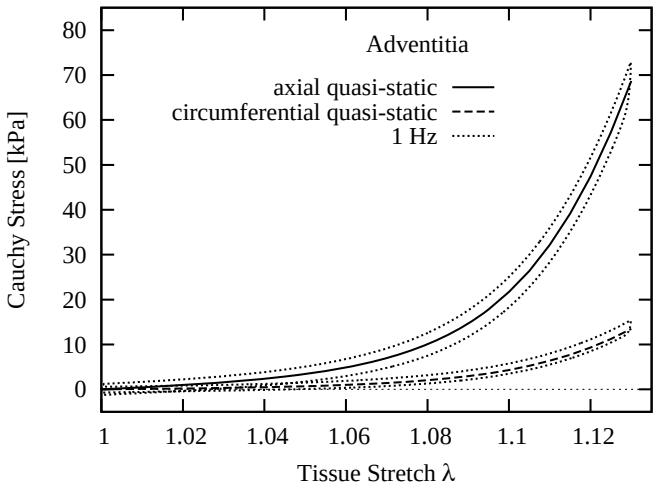

Fig. 4. – Cauchy stress *vs.* stretch for loading of adventitial tisue in axial and circumferential direction. The curves show the equilibrium responses and the solutions for stretch controlled triangular-shaped loading/unloading at 1 Hz. Anisotropy and hysteretic behaviour are observed. Material parameters: $\mu = 1.0$, $c = 50.0\,\mathrm{MPa}$, $k_1 = 45.0\,\mathrm{kPa}$, $k_2 = 50.0$, $\eta_0 = 30.0\,\mathrm{kPas}$, $d = 150.0$.

In application to layers of the arterial wall, which are characterised by distinct fibre distributions, the model predicts the typical anisotropic and J-shaped stress-stretch characteristics under quasi-static conditions as well as hysteresis in cyclic loading. Notwithstanding, with the proposed method, the particular viscoelastic characteristics of various other soft tissues can be accounted for by appropriate representations of the strain-energy, viscosity and fibre distribution functions. Hence, the presented general approach delivers an excellent framework to model the particular anisotropic viscoelastic behaviour of a broad variety of soft biological tissues.

REFERENCES

[1] Fung Y. C., *Biomechanics: Mechanical Properties of Living Tissues*, 2nd ed. (Springer, New York) 1993.
[2] Bischoff J. E., Arruda E. M. and Grosh K., *Biomech. Model. Mechanobiol.*, **3** (2004) 56.
[3] Holzapfel G. A. and Gasser T. C., *Comput. Methods Appl. Mech. Eng.*, **190** (2001) 4379.
[4] Le Tallec P., Rahier C. and Kaiss A., *Comput. Methods Appl. Mech. Eng.*, **109** (1993) 233.
[5] Peña E. *et al.*, *Int. J. Solids Struct.*, **44** (2007) 760.
[6] Nguyen T. D., Jones R. E. and Boyce L., *Int. J. Solids Struct.*, **44** (2007) 8366.
[7] Atkinson T. S., Haut R. C. and Altiero N. J., *J. Biomech. Eng.*, **119** (1997) 400.
[8] Ehlers W. and Markert B., *J. Biomech. Eng.*, **123** (2001) 418.
[9] De Vita R. and Slaughter W. S., *Int. J. Solids Struct.*, **43** (2006) 1561.
[10] Limbert G. and Middleton J., *Int. J. Solids Struct.*, **41** (2004) 4237.
[11] Pioletti D. P. *et al.*, *J. Biomech.*, **31** (1998) 753.

[12] Puxkandl R. *et al.*, *Philos. Trans. R. Soc. London, Ser. B*, **357** (2002) 191.
[13] Ehret A. E., Itskov M. and Weinhold G., *Proceedings of the IUTAM Symposium on Cellular, Molecular and Tissue Mechanics, 2008*, edited by Garikipati K. and Arruda E. M. (Springer), in press.
[14] Lanir Y., *J. Biomech.*, **12** (1979) 423; **16** (1983) 1.
[15] Miehe C., Göktepe S. and Lulei F., *J. Mech. Phys. Solids*, **52** (2004) 2617.
[16] Caner F. C. and Carol I., *J. Biomech. Eng.*, **128** (2006) 419.
[17] Ehret A. E., Itskov M. and Schmid H., submitted to *Int. J. Numer. Meth. Eng.*
[18] Heo S. and Xu Y., *Math. Comput.*, **70** (2001) 269.
[19] Holzapfel G. A., Gasser T. C. and Ogden R. W., *J. Elasticity*, **61** (2000) 1.
[20] Finlay H. M., McCullogh L. and Canham P. B., *J. Vasc. Res.*, **32** (1995) 301.